

Climate of the Past Discussions is the access reviewed discussion forum of *Climate of the Past*

Information on the early Holocene climate constrains the summer sea ice projections for the 21st century

H. Goosse, E. Driesschaert, T. Fichefet, and M.-F. Loutre

Université Catholique de Louvain, Institut d’Astronomie et de Géophysique G. Lemaître,
Chemin du Cyclotron, 2, 1348 Louvain-la-Neuve, Belgium

Received: 15 August 2007 – Accepted: 23 August 2007 – Published: 24 August 2007

Correspondence to: H. Goosse (hgs@astr.ucl.ac.be)

CPD

3, 999–1020, 2007

Summer sea ice during the early Holocene

H. Goosse et al.

Title Page

Abstract

Introduction

Conclusions

References

Tables

Figures

⏪

⏩

◀

▶

Back

Close

Full Screen / Esc

Printer-friendly Version

Interactive Discussion

EGU

Abstract

The summer sea ice extent strongly decreased in the Arctic over the last decades. This decline is very likely to continue in the future but uncertainty on projections is very large. An ensemble of experiments with the climate model LOVECLIM using 5 different parameter sets has been performed to show that summer sea ice changes for the early Holocene and for the 21st century are strongly linked, allowing to reduce this uncertainty. Using the limited information presently available for the early Holocene, simulations presenting very large changes for the 21st century could reasonably be rejected. On the other hand, simulations displaying low to moderate changes during the second half of the 20th century are not consistent with recent observations. Using this evidence based on observations during both the early Holocene and the last decades, the most realistic projection indicates a nearly disappearance of the sea ice at the end of the 21st century for a moderate increase in atmospheric greenhouse gas concentrations. For a faster increase in those concentrations, the Arctic Ocean would become almost ice-free in summer as early as 2060 AD.

1 Introduction

Over the last 30 years, corresponding to the period of satellite microwave observations, the Arctic sea ice extent has decreased at a mean rate of about $0.3 \times 10^6 \text{ km}^2$ per decade (Lemke et al., 2007). The summer decline was found to be even larger, with a reduction of $0.6 \times 10^6 \text{ km}^2$ per decade (Lemke et al., 2007; Stroeve et al., 2007). Those recent observed changes have led to considerable attention on the model projections of summer sea ice changes, the eventuality of a seasonally ice-free Arctic before the end of this century being one the strongest image associated with future climate warming (e.g. Arzel et al., 2006; Holland et al., 2006; Zhang and Walsh, 2006; Meehl et al., 2007; Serreze et al., 2007; Schiermeier, 2007).

All the simulations performed in the framework of the Intergovernmental Panel for

CPD

3, 999–1020, 2007

Summer sea ice during the early Holocene

H. Goosse et al.

Title Page

Abstract

Introduction

Conclusions

References

Tables

Figures

◀

▶

◀

▶

Back

Close

Full Screen / Esc

Printer-friendly Version

Interactive Discussion

EGU

Climate Change Fourth Assessment Report (IPCC AR4) show that the Arctic sea ice decline will continue during the whole 21st century in response to the increase in the concentrations of atmospheric greenhouse gases (Arzel et al., 2006; Zhang and Walsh, 2006; Meehl et al., 2007; Serreze et al., 2007). However, there is more than a factor three in the estimates of the future trend between the different models, even using an identical scenario for the future evolution of the concentrations of atmospheric greenhouse gases (Arzel et al., 2006; Zhang and Walsh, 2006; Meehl et al., 2007; Serreze et al., 2007). Reducing the projections uncertainties is thus a major objective of the climate modelling community and a major challenge.

It is customary to assess the quality of models by comparing their output with recent observations. In particular, the models not able to reproduce sufficiently well the observed mean Arctic ice extent at the end of the 20th century were discarded in a number of recent analyses (e.g., Arzel et al., 2006, Stroeve et al., 2007). However, the decision to reject a model is partly arbitrary and not consistent across papers (Arzel et al., 2006; Stroeve et al., 2007). Furthermore, the relevance of rejection criteria may also be called into question because it has been hard to find strong relationships between the model characteristics simulated at the end of the 20th century and the decrease in sea ice extent obtained during the 21st century (Arzel et al., 2006; Holland and Bitz, 2003; Flato, 2004).

The observed decrease rate in Arctic sea ice extent over the last decades provides another test case for models (Arzel et al., 2006; Zhang and Walsh, 2006; Meehl et al., 2007; Serreze et al., 2007; Stroeve et al., 2007). In particular, it is shown in a recent study (Stroeve et al., 2007) that no simulation performed in the framework of the IPCC AR4 is able to reproduce the observed decline in summer ice extent over the last 53 years. This provides evidence that the models underestimate the response of the sea ice to rising concentration of greenhouse gases in the atmosphere. However, there is still the possibility that the recent decline is a very rare event of natural variability that is not captured by the relatively small ensemble of simulations presently available (Stroeve et al., 2007).

Summer sea ice during the early Holocene

H. Goosse et al.

[Title Page](#)[Abstract](#)[Introduction](#)[Conclusions](#)[References](#)[Tables](#)[Figures](#)[◀](#)[▶](#)[◀](#)[▶](#)[Back](#)[Close](#)[Full Screen / Esc](#)[Printer-friendly Version](#)[Interactive Discussion](#)

Summer sea ice during the early Holocene

H. Goosse et al.

Title Page

Abstract

Introduction

Conclusions

References

Tables

Figures

◀

▶

◀

▶

Back

Close

Full Screen / Esc

Printer-friendly Version

Interactive Discussion

Additional constraints on the model behaviour could be provided by simulations devoted to the more distant past such as the mid-Holocene (6 kyr BP, i.e. 6000 years before present) or the last glacial maximum (21 kyr BP) (e.g., Crucifix, 2006; Masson-Delmotte et al., 2006). However, only the past periods for which the external forcing is well known, a reasonably large amount of data is available and the variable of interest displays large changes compared to the recent past are expected to provide a stringent test of the model.

The early Holocene is potentially a good candidate to constrain the analysis of the response of the Arctic summer ice cover to a radiative perturbation. Indeed, the insolation in June at 8 kyr BP was much larger than in recent decades (Berger, 1978), the differences reaching $+40 \text{ W/m}^2$ in June northward of 65° N (Fig. 1). Seemingly consistent with this forcing, the various geological reconstructions and model simulations for this period display higher summer temperatures and a lower sea ice extent at high latitudes (e.g., Koç et al., 1993; Duplessy et al., 2001; Vavrus and Harrison, 2003; Braconnot et al., 2007). Here we show how model simulations over this period could help us in reducing the uncertainties in the projections of the decline of the summer Arctic ice extent during the 21st century. Specifically, we have selected the period around 8 kyr BP because the sea ice changes are larger than for the most classical mid-Holocene period (e.g., Renssen et al., 2005). In this framework, we performed simulations with the three-dimensional climate model LOVECLIM (Driesschaert et al., 2007) using five different sets of parameters (called E1 to E5, Appendix A), chosen to explore the uncertainty range in these parameters as in Murphy et al. (2004) and Stainforth et al. (2005). Our simulations cover the period from the early Holocene to 2100 AD. For the period 1850–2100 AD, an ensemble of simulations with slightly different initial conditions is performed to estimate the model internal variability for each parameter set (see Sect. 2). As a consequence, we provide here controlled experiments with the same model version spanning the whole time period selected and using the same forcing for all the three-dimensional model parameter sets chosen.

2 Model description and experimental design

LOVECLIM is a three-dimensional Earth system model of intermediate complexity that includes representations of the atmosphere, the ocean and sea ice, the land surface, the ice sheets and the carbon cycle. In the present study, the ice sheet and carbon cycle components are not activated and will thus not be described here. The atmospheric component is ECBILT2 (Opseegh et al., 1998), a T21, 3-level quasi-geostrophic model. The oceanic component is CLIO3 (Goosse and Fichefet, 1999), which is made up of an ocean general circulation model coupled to a comprehensive thermodynamic-dynamic sea ice model. Its horizontal resolution is 3° by 3° , and there are 20 levels in the ocean. ECBILT-CLIO is coupled to VECODE, a vegetation model that simulates the dynamics of two main terrestrial plant functional types, trees and grasses, as well as desert (Brovkin et al., 2002). Its resolution is the same as the one of ECBILT. More information about the model and a complete list of references is available at the following address: <http://www.astr.ucl.ac.be/index.php?page=LOVECLIM%40Description>.

The model version used here is LOVECLIM1.1. Three main improvements have been incorporated in this version compared to LOVECLIM1.0 (Driesschaert et al., 2007). First, the land surface scheme has been modified (see http://www.astr.ucl.ac.be/ASTER/doc/E_AR_SDCS01A_v2.pdf) in order to take into account the impact of the changes in vegetation on the evaporation (transpiration) and on the bucket depth (i.e. the maximum water that can be hold in the soil). Second, the emissivity, which was the same for all the surfaces in LOVECLIM1.0, is now different for land, ocean and sea ice. Third, in order to reduce the artificial vertical diffusion in the ocean caused by numerical noise, the Coriolis term is now treated in a fully implicit way in the equation of motion for the ocean, while a semi-implicit scheme was used in LOVECLIM1.0 (see also Appendix A).

In order to obtain the five model parameter sets considered here, different parameter values have been selected, each of them being in the range of uncertainty of the parameter considered (Appendix A). The goal is, on the one hand, to produce rea-

CPD

3, 999–1020, 2007

Summer sea ice during the early Holocene

H. Goosse et al.

Title Page

Abstract

Introduction

Conclusions

References

Tables

Figures

◀

▶

◀

▶

Back

Close

Full Screen / Esc

Printer-friendly Version

Interactive Discussion

EGU

sonable simulations of the present-day climate (Table 2), which have similar qualities when compared to the observations in all the regions of the world and for a wide range of variables (surface temperature, precipitation, oceanic and atmospheric circulations, sea ice concentration, radiative exchanges at the top of the atmosphere). On the other hand, these model parameter sets must lead to clearly contrasted model responses to a perturbation. In particular, the climate sensitivities cover a range from 1.6 to 3.8 K (Table 1). The climate sensitivity is defined here as the global surface temperature change after 1000 years in an experiment performed with LOVECLIM in which the CO₂ concentration increases from pre-industrial level by 1% per year and is maintained constant after 70 years of integration when it reaches a value equal to two times the pre-industrial level. Such a simulation is a classical benchmark to compare different model responses to a radiative perturbation.

Three types of simulations, launched for the five parameter sets, are conducted with the model. First, a quasi-equilibrium simulation with a constant forcing corresponding to pre-industrial conditions is performed with the CO₂, CH₄ and N₂O concentrations in the atmosphere respectively set to 277.6 ppmv, 628.2 ppbv, 267.4 ppbv, respectively. Second, a quasi-equilibrium simulation is carried out with orbital parameters and greenhouse gas concentrations corresponding to the 8 kyr BP conditions. In this experiment CO₂, CH₄ and N₂O concentration concentrations are maintained constant at values of 260.6 ppmv, 701.5 ppbv, 267.4 ppbv, respectively. Third, a transient simulation is made from 8kyr BP to year 2100 AD, starting from the quasi-equilibrium obtained for 8 kyr BP. Between 8 kyr BP and 1 AD, the only forcings applied are insolation and greenhouse ones as in Renssen et al. (2005). After 1 AD, in addition to those forcings, the variations in the total solar irradiance, the impact of big volcanic eruptions as well as the role of land-use changes (starting in 1000 AD) and of the increase in aerosol load (starting in 1850 AD) are taken into account as in Goosse et al. (2005). For the 21st century, the forcing follows the scenario IPCC Special Report on Emissions Scenarios (SRES) B1, in which the CO₂ concentration reaches 540 ppmv in 2100 AD. For each model parameter set, in order to sample the internal variability of the model, 5 ensem-

Summer sea ice during the early Holocene

H. Goosse et al.

Title Page

Abstract

Introduction

Conclusions

References

Tables

Figures

◀

▶

◀

▶

Back

Close

Full Screen / Esc

Printer-friendly Version

Interactive Discussion

ble members are performed (i.e. a total of 25 simulations) over the period 1851–2100 AD. To do so, we have introduced a very small perturbation on the quasi-geostrophic potential vorticity the 1 January 1851. In all those experiments, the ice sheet topography is maintained at its present value. For the early Holocene, sensitivity experiments performed with an earlier version of the model (Renssen et al., 2005) have shown that neglecting the influence of the remnant of the Laurentide ice sheet has only a marginal, regional impact at that time and this approximation should thus not influence strongly our results.

3 Results

By construction, all the simulations provide rather similar Arctic sea ice extent for pre-industrial conditions and the late 20th century (Fig. 2, Table 1). Each of them has its own biases, with magnitude of the same order as those observed in state-of-the-art atmosphere-ocean general circulation models (e.g., Arzel et al., 2006, Zhang and Walsh 2006). For instance, all the simulations have a general tendency to overestimate the ice concentration in the Northern part of the Baffin Bay and on the Shelf of the East Siberian Sea during the late 20th century.

By contrast, Arctic summer sea ice extent at 8 kyr BP clearly varies across the different simulations, emphasizing a large dependence of model sensitivity to changes in model parameters. For E5, ice only remains in summer between the north coast of Greenland and the North Pole while ice persists for E1 in all the Arctic Basin and even covers a large part of the Siberian continental shelves. No synthesis of summer sea ice margin location is available for the early Holocene yet but the various reconstructions consistently show a reduced summer ice cover and an oceanic warming for this period, in particular in the Greenland and Barents Seas (e.g., Koç et al, 1993; Duplessy et al., 2001, Bennike, 2004). Some observations even suggest a higher amount of open water (leads) in the Central Arctic during this period (Nørgaard-Pedersen et al., 1998). In the western Arctic Ocean, the signal is less clear with probably smaller

Summer sea ice during the early Holocene

H. Goosse et al.

Title Page

Abstract

Introduction

Conclusions

References

Tables

Figures

◀

▶

◀

▶

Back

Close

Full Screen / Esc

Printer-friendly Version

Interactive Discussion

changes than in the European sector (Dyke et al., 2001, de Vernal et al., 2005). As a consequence, E5 very likely overestimates the reduction in ice extent north of the Canadian Archipelago for the early Holocene. It is worth mentioning that, in this experiment, the summer sea ice extent reaches $4.8 \times 10^6 \text{ km}^2$ at 6 kyr BP, i.e. a value very close to the mean for the period 1980–2000 AD (Table 2). This demonstrates that the signal is much stronger at 8 kyr BP than at 6 kyr BP, providing a much stronger constraint for the model. On the other hand, none of E1–E4 can clearly be rejected on the basis of 8 kyr BP observations.

All the simulations display a decrease in summer sea ice extent throughout the 20th and 21st centuries but with very different magnitudes (Fig. 3). In fact, the range covered by our simulations over this period is even larger than the one given by the IPCC AR4 (Stroeve et al., 2007). Our simulations performed with different model parameter sets provide thus a good sample of the present uncertainties in future projections. Compared to observations covering the second half of the 20th century and the beginning of the 21st century, E1, E2 and, to a smaller extent, E3 seriously underestimate the decline in summer ice extent (Table 2). The size of the ensemble of simulation performed for each parameter set is still relatively small to obtain reliable statistics of internal variability. Nevertheless, the simulated mean trend is smaller than the observed trend for the period 1953–2006 AD by more than 2 standard deviations over the ensemble, for those three parameters sets (Table 2). We thus consider the eventuality that the observed decline was due to a rare event of natural variability as highly unlikely and we prefer the more reasonable hypothesis that E1, E2 and E3 are incompatible with the observed record.

Figures 2 and 3 suggest evidence of strong consistency between past and future summer sea ice changes across the different parameter sets. Specifically, the summer ice extent averaged over the period 2040–2060 AD is very close to 1.5 times the one simulated for 8 kyr BP for all the model parameter sets (Fig. 4). As sea ice almost disappears in summer after 2050 AD for E5, the comparison becomes meaningless for this parameter set, but the strong relationship with the ice extent simulated at 8 kyr

Summer sea ice during the early Holocene

H. Goosse et al.

Title Page

Abstract

Introduction

Conclusions

References

Tables

Figures

◀

▶

◀

▶

Back

Close

Full Screen / Esc

Printer-friendly Version

Interactive Discussion

BP appears also valid for the averaged ice extent over the periods 2060–2080 AD and 2080–2100 AD (not shown).

4 Conclusions

The robust link between the simulated decrease in the Arctic summer sea ice extent during the 21st century and for 8 kyr BP is obtained for a wide range of model responses despite the very different forcings changes during the two periods. Indeed, the forcing is slowly varying for the early Holocene and has a very strong seasonal cycle. By contrast, the forcing changes rapidly over the 20th and 21st centuries, the climate system being in a clearly transient state, and the forcing anomaly is more homogeneously distributed for the different seasons.

Information about the state of the climate system during the early Holocene could thus help us in reducing our uncertainties on the future decline of the Arctic ice cover. The available reconstructions are still very fragmentary and additional observations are required in order to obtain precise and reliable projections. In particular, new oceanic cores obtained in the framework of the International Polar Year will be particularly useful (e.g., <http://classic.ipy.org/development/eoi/details.php?id=786>).

Nevertheless, the small number of available reconstructions still allowed us to consider that the model results for one of our parameter sets (E5) are not in agreement with observations, as the summer sea ice cover nearly disappears under early Holocene conditions. In addition, the analysis of the simulated decrease in ice extent over the last decades shows that simulations presenting a weak response are not compatible with the observed decline of the summer ice extent during this period (E1, E2 and E3). From those evidences, the future projection obtained using the remaining parameter set (E4) appears the most reliable. For the relatively moderate scenario SRES B1, this E4 simulation displays a reduction in summer sea ice extent larger than 60% in 2050 and a nearly disappearance of the summer Arctic ice pack at the end of the 21st century. For a more pessimistic scenario like SRES A2, in which the atmospheric CO₂

Summer sea ice during the early Holocene

H. Goosse et al.

Title Page

Abstract

Introduction

Conclusions

References

Tables

Figures

⏪

⏩

◀

▶

Back

Close

Full Screen / Esc

Printer-friendly Version

Interactive Discussion

Summer sea ice during the early Holocene

H. Goosse et al.

Title Page

Abstract

Introduction

Conclusions

References

Tables

Figures

◀

▶

◀

▶

Back

Close

Full Screen / Esc

Printer-friendly Version

Interactive Discussion

concentration in the atmosphere reaches about 830 ppmv in 2100, the decline of the Arctic sea ice in summer would be even faster. Consequently, the Arctic would become almost ice-free in summer in 2060 AD in this scenario (Fig. 5). Those values are below the range (multimodel mean ± 1 standard deviation) provided by the IPCC AR4 (Meehl et al., 2007), indicating that this recent report likely provides too conservative projections of the future changes in summer sea ice extent for the Arctic.

Appendix A

The five model parameter sets selected

| Name | λ_2 (1) | λ_4 (1) | <i>amplw</i> (2) | <i>explw</i> (2) | <i>albocef</i> (3) | <i>albice</i> (4) | <i>avkb</i> (5) |
|------|-----------------|-----------------|------------------|------------------|--------------------|-------------------|-----------------|
| E1 | 0.125 | 0.070 | 1.00 | 0.3333 | 1.000 | 0 | 1.0 (6) |
| E2 | 0.125 | 0.070 | 1.00 | 0.4 | 0.900 | 0 | 1.5 |
| E3 | 0.131 | 0.071 | 1.00 | 0.5 | 0.950 | 0 | 2.5 |
| E4 | 0.131 | 0.071 | 1.10 | 0.5 | 0.900 | 0 | 2.5 |
| E5 | 0.131 | 0.071 | 1.30 | 0.5 | 1.050 | 0.02 | 2.0 |

(1) λ_2 and λ_4 are two parameters applied in the Rayleigh damping term of the equation of the quasi-geostrophic potential vorticity. λ_2 corresponds to the 500–800 hPa layer of the model while λ_4 corresponds 200–500 hPa layer (see equation 1 of Opsteegh et al., 1998, and equation 11 of Haarsma et al., 1996).

(2) The simple longwave radiative scheme of LOVECLIM is based on an approach termed the Green's function method (Chou and Neelin, 1996; Schaeffer et al., 1998). The scheme could be briefly represented for clear-sky conditions by the following for-

mula for all the model levels:

$$Flw = Fref + FG(T', GHG') + G1 * amplw * (q') **explw$$

where Flw is the longwave flux, $Fref$ a reference value of the flux when temperature, humidity and the concentrations of greenhouse gases are equal to the reference values, FG a function, not explicitly described here, allowing to compute the contribution associated with the anomalies compared to this reference in the vertical profile of temperature (T') and in the concentrations of the various greenhouse gases in the atmosphere (GHG'). The last term represents the anomaly in the longwave flux due to the anomaly in humidity q' . The coefficients $Fref$, $G1$ and those included in the function FG are spatially dependent. All the terms have been calibrated to follow as closely as possible a complex general circulation model longwave scheme (Schaeffer et al., 1998), but large uncertainties are of course related to this parameterization, in particular as the model only computes one mean relative humidity between the surface and 500 hPa, the atmosphere above 500 hPa being supposed to be completely dry.

(3) The albedo of the ocean in LOVECLIM depends on the season and of the location. At each time step, it is multiplied by $albcoef$ in the experiments analysed here. For a typical albedo of the ocean of 0.06, using a value of 1.05 for $albcoef$ increases the value of the albedo to 0.063.

(4) The albedo of sea ice is based on the scheme of Shine and Henderson-Sellers (1985), which uses different values for the albedo of dry snow, melting snow, frozen ice and melting ice. For thin ice the albedo is also dependent on the ice thickness. If $albice$ is different from zero in the experiments discussed here, the value of the albedo in the model is increased by $albice$ for all the snow and ice types.

(5) As explained in detail in Goosse et al. (1999), the minimum vertical diffusivity in the ocean follows a vertical profile similar to the one proposed in Bryan and Lewis (1979). The coefficient $avkb$ is a scaling factor that multiplies the minimum values of the vertical diffusivity at all depths. A value of $avkb$ of 1 (1.5, 2, 2.5) corresponds to a minimum background vertical diffusivity in the thermocline of $10^{-5} \text{ m}^2/\text{s}$ (1.510^{-5} , 2×10^{-5} , $2.5 \times 10^{-5} \text{ m}^2/\text{s}$).

Summer sea ice during the early Holocene

H. Goosse et al.

Title Page

Abstract

Introduction

Conclusions

References

Tables

Figures

◀

▶

◀

▶

Back

Close

Full Screen / Esc

Printer-friendly Version

Interactive Discussion

Summer sea ice during the early Holocene

H. Goosse et al.

Title Page

Abstract

Introduction

Conclusions

References

Tables

Figures

◀

▶

◀

▶

Back

Close

Full Screen / Esc

Printer-friendly Version

Interactive Discussion

(6) In LOVECLIM1.1, the Coriolis term in the equation of motion is computed in a totally implicit way because the semi-implicit scheme used for this term in LOVECLIM1.0 induced too much numerical noise. The older scheme has been kept here in E1 only, in order to have an easier comparison with the results of LOVECLIM1.0. Because of the larger implicit diffusion associated with this scheme, a lower value of the explicit diffusion is applied in E1.

Acknowledgements. H. Goosse is Research Associate with the Fonds National de la Recherche Scientifique (FNRS-Belgium). This work is supported by the FNRS and by the Belgian Federal Science Policy Office, Research Program on Science for a Sustainable Development. We would like to thank M. Crucifix for his help in the experimental design and for a careful reading of the manuscript.

References

- Arzel, O., Fichfet, T. and Goosse, H.: Sea ice evolution over the 20th and 21st centuries as simulated by current AOGCM, *Ocean Model.*, 12, 401–415, 2006.
- Bennike, O.: Holocene sea-ice variations in Greenland: onshore evidence, *Holocene*, 14, 607–613, 2004.
- Berger A. L.: Long-term variations of daily insolation and Quaternary climatic changes, *J. Atmos. Sci.*, 35, 2363–2367, 1978.
- Braconnot P., Otto-Bliesner, B., Harrison, S., Joussaume, S., Peterchmitt, J.-Y., Abe-Ouchi, A., Crucifix, M., Driesschaert, E., Fichfet, Th., Hewitt, C. D., Kageyama, M., Kitoh, A., Loutre, M.-F., Marti, O., Merkel, U., Ramstein, G., Valdes, P., Weber, S. L., Yu, Y., and Zhao, Y.; Results of PMIP2 coupled simulations of the Mid-Holocene and Last Glacial Maximum Part 2: feedbacks with emphasis on the location of the ITCZ and mid- and high latitudes heat budget, *Clim. Past*, 3, 279–296, 2007, <http://www.clim-past.net/3/279/2007/>.
- Brovkin, V., Bendtsen, J., Claussen, M., Ganopolski, A., Kubatzki, C., Petoukhov, V., and Andreev, A.: Carbon cycle, vegetation and climate dynamics in the Holocene: experiments with the CLIMBER-2 model, *Global Biogeochem. Cycles*, 16, 1139, doi:10.1029/2001GB001662, 2002.

- Bryan, K. and Lewis, L.J.: A water mass model of the world ocean, *J. Geophys. Res.*, 84, 2503–2517, 1979.
- Chou, C. and Neelin, J. D.: Linearization of a long-wave radiation scheme for intermediate tropical atmospheric model, *J. Geophys. Res.*, 101, 15 129–15 145, 1996.
- 5 Comiso, J.: Bootstrap sea ice concentrations for NIMBUS-7 SMMR and DMSP SSM/I, June to September 2001. Boulder, CO, USA, National Snow and Ice Data Center Digital media, 1999 updated 2005.
- Crucifix, M.: Does the Last Glacial Maximum constrain climate sensitivity? *Geophys. Res. Lett.*, 33, L18701, doi:10.1029/2006GL027137, 2006.
- 10 de Vernal, A., Hilaire-Marcel, C., and Darby, D. A.: Variability of the ice cover in the Chukchi Sea (western Arctic Ocean) during the Holocene. *Paleoceanography*, 20, PA4018, doi:10.1029/2005PA001157, 2005.
- Driesschaert, E., Fichet, T., Goosse, H., Huybrechts, P., Janssens, I., Mouchet, A., Munhoven, G., Brovkin, V., and Weber, S. L.: Modeling the influence of Greenland ice sheet melting on the Atlantic meridional overturning circulation during the next millennia, *Geophys. Res. Lett.* 34, L10707, doi:10.1029/2007GL029516, 2007.
- 15 Duplessy, J. C., Ivanova, E., Murdmaa, I., Paterné, M., and Labeyrie L.: Holocene paleoceanography of the northern Barents Sea and variations of the northward heat transport by the Atlantic Ocean, *Boreas*, 30, 2–16, 2001.
- 20 Dyke, A. S. and Saville, J. M.: Holocene history of the Bering Sea bowhead whale (*Balaena mysticetus*) in its Beaufort Sea summer grounds off southwestern Victoria Island, western Canadian Arctic, *Quaternary Res.*, 55, 371–379, 2001.
- Flato, G. M.: Sea-ice and its response to CO₂ forcing as simulated by global climate models, *Clim. Dyn.*, 23, 229–241, 2004.
- 25 Goosse, H. and Fichet, T.: Importance of ice-ocean interactions for the global ocean circulation: a model study, *J. Geophys. Res.*, 104, 23 337–23 355, 1999.
- Goosse, H., Renssen, H., Timmermann, A., and Bradley, R. S.: Internal and forced climate variability during the last millennium: a model-data comparison using ensemble simulations, *Quat. Sciences Rev.*, 24, 1345–1360, 2005.
- 30 Goosse, H., Deleersnijder, E., Fichet, T., and England, M. H.: Sensitivity of a global coupled ocean-sea ice model to the parameterization of vertical mixing, *J. Geophys. Res.*, 104, 13 681–13 695, 1999.
- Haarsma, R. J., Selten, F. M., Opsteegh, J. D., Lenderink, G., and Liu, Q.: ECBILT, a cou-

Summer sea ice during the early HoloceneH. Goosse et al.

[Title Page](#)[Abstract](#)[Introduction](#)[Conclusions](#)[References](#)[Tables](#)[Figures](#)[◀](#)[▶](#)[◀](#)[▶](#)[Back](#)[Close](#)[Full Screen / Esc](#)[Printer-friendly Version](#)[Interactive Discussion](#)

- pled atmosphere ocean sea-ice model for climate predictability studies. KNMI, De Bilt, The Netherlands, 31 pp., 1996.
- Holland, M. M. and Bitz, C. M.: Polar amplification of climate change in coupled models, *Clim. Dyn.*, 21, 221–232, 2003.
- 5 Holland, M. M., Bitz, C. M., and Tremblay, B.: Future abrupt reductions in the summer Arctic sea ice, *Geophys. Res. Lett.*, 33, L23503, doi:10.1029/2006GL028024, 2006.
- Koç, N., Jansen E., and Hafliðason, H.: Paleoceanographic reconstructions of surface ocean conditions in the Greenland, Iceland and Norwegian seas through the last 14 ka based on diatoms, *Quat. Sciences. Rev.*, 12, 115–140, 1993.
- 10 Lemke, P., Ren, J., Alley, R. B., et al.: Observations: Changes in Snow, Ice and Frozen Ground, in: *Climate Change 2007: The Physical Science Basis. Contribution of Working Group I to the Fourth Assessment Report of the Intergovernmental Panel on Climate Change*, edited by: Solomon, S., Qin, D., Manning, M., Chen, Z., Marquis, M., Averyt, K. B., Tignor, M., and Miller, H. L., Cambridge Univ. Press, Cambridge, 2007.
- 15 Masson-Delmotte, V., Kageyama, M., Braconnot, P., Charbit, S., Krinner, G., Ritz, C., Guilyardi, E., Jouzel, J., Abe-Ouchi, A., Crucifix, M., Gladstone, R. M., Hewitt, C. D., Kitoh, A., LeGrande, A. N., Marti, O., Merkel, U., Motoi, T., Ohgaito, R., Otto-Bliesner, B., Peltier, W. R., Ross, I., Valdes, P. J., Vettoretti, G., Weber, S. L., Wolk, F., and Yu, Y.: Past and future polar amplification of climate change: climate model intercomparisons and ice-core constraints, *Clim. Dyn.*, 27, 437–440, 2006.
- 20 Meehl, G. A., Stocker, T. F., Collins, W. D., et al.: Global Climate Projections, in: *Climate Change 2007: The Physical Science Basis. Contribution of Working Group I to the Fourth Assessment Report of the Intergovernmental Panel on Climate Change*, edited by: Solomon, S., Qin, D., Manning, M., Chen, Z., Marquis, M., Averyt, K. B., Tignor, M., and Miller, H. L., Cambridge Univ. Press, Cambridge, 2007.
- 25 Murphy, J. M., Sexton, D. M. H., Barnett, D. N., Jones, G. S., Webb, M. J., Collins, M., and Stainforth, D. A.: Quantification of modelling uncertainties in a large ensemble of climate change simulations, *Nature*, 430, 768–772, 2004.
- Nørgaard-Pedersen, N., Spielhagen, R. F., Thiede, J., and Kassens, H.: Central Arctic surface ocean environment during the past 80000 years, *Paleoceanography*, 13, 193–204, 1998.
- 30 Opsteegh, J. D., Haarsma, R. J., Selten, F. M., and Kattenberg, A.: ECBILT: A dynamic alternative to mixed boundary conditions in ocean models, *Tellus*, 50A, 348–367, 1998.
- Renssen, H., Goosse, H., Fichet, T., Brovkin, V., Driesschaert, E., and Wolk, F.: Simulating

Summer sea ice during the early Holocene

H. Goosse et al.

Title Page

Abstract

Introduction

Conclusions

References

Tables

Figures

◀

▶

◀

▶

Back

Close

Full Screen / Esc

Printer-friendly Version

Interactive Discussion

the Holocene climate evolution at northern high latitudes using a coupled atmosphere-sea ice-ocean-vegetation mode, *Clim. Dyn.*, 24, 23–43, 2005.

Schaeffer, M., Selten, F., and van Dorland, R.: Linking Image and ECBILT. National Institute for public health and the environment (RIVM), Bilthoven, The Netherlands, Report no 4815008008, 1998.

Schiermeier, Q.: The new face of the Arctic, *Nature*, 446, 133–135, 2007.

Serreze, M. C., Holland, M. M., and Stroeve, J.: Perspectives on the Arctic's shrinking sea-ice cover, *Science*, 315, 1533–1536, 2007.

Shine, K. P.: Henderson-Sellers, A.: The sensitivity of a thermodynamic sea ice model to changes in surface albedo parameterization, *J. Geophys. Res.*, 90, 2243–2250, 1985.

Stainforth, D. A., Aina, T., Christensen, C., Collins, M., Faull, N., Frame, D. J., Kettleborough, J. A., Knight, S., Martin, A., Murphy, J. M., Piani, C., Sexton, D., Smith, L. A., Spicer, R. A., Thorpe, A. J., and Allen M. R.: Uncertainty in predictions of the climate response to rising levels of greenhouse gases, *Nature* 433, 403–406, 2005.

Stroeve, J., Holland, M. M., Meier, W., Scambos, T., and Serreze, M.: Arctic sea ice decline: Faster than forecast, *Geophys. Res. Lett.*, 34, L09501, doi:10.1029/2007GL029703, 2007.

Vavrus, S. and Harrison, S. P.: The impact of sea-ice dynamics on the Arctic climate system, *Clim. Dyn.*, 20, 741–757, 2003.

Zhang, X. and Walsh, J. E.: Toward a seasonally ice-covered Arctic Ocean: scenarios from the IPCC AR4 model simulations, *J. Clim.*, 19, 1730–1747, 2006.

CPD

3, 999–1020, 2007

Summer sea ice during the early Holocene

H. Goosse et al.

Title Page

Abstract

Introduction

Conclusions

References

Tables

Figures

◀

▶

◀

▶

Back

Close

Full Screen / Esc

Printer-friendly Version

Interactive Discussion

Summer sea ice during the early Holocene

H. Goosse et al.

Title Page

Abstract

Introduction

Conclusions

References

Tables

Figures

◀

▶

◀

▶

Back

Close

Full Screen / Esc

Printer-friendly Version

Interactive Discussion

Table 1. Some characteristics of the various experiments.

| Name | Climate sensitivity ¹ | Max. MOC2 | Min ice extent ³ | Max ice extent ³ |
|------|----------------------------------|-----------|-----------------------------|-----------------------------|
| E1 | 1.6 | 28.2 | 9.4 | 14.7 |
| E2 | 2.1 | 25.9 | 8.8 | 15.3 |
| E3 | 2.6 | 25.5 | 8.0 | 14.5 |
| E4 | 3.2 | 24.8 | 8.5 | 15.2 |
| E5 | 3.8 | 23.5 | 7.4 | 14.7 |

¹ The climate sensitivity is defined here as the temperature (in K) change after 1000 year in an experiment performed with LOVECLIM in which the CO₂ concentration increases from pre-industrial level by 1% per year and is maintained constant after 70 years of integration when it reaches a value equal to two times the pre-industrial value.

² Maximum of the meridional overturning circulation (MOC) in the North Atlantic (in Sv=10⁶ m³/s).

³ Minimum and maximum sea ice extents in the Northern Hemisphere for pre-industrial conditions in 10⁶ km². The ice extent is defined as the total oceanic area with an ice concentration of at least 15%.

Summer sea ice during the early Holocene

H. Goosse et al.

Table 2. Minimum sea ice extent (in 10^6 km²) in the Northern Hemisphere for different periods.

| Name | Min ice extent ¹ preind | Min ice extent 8 BP | Min ice extent 1980–2000 | Min ice extent 2040–2060 ² | Trend over the period 1979–2006 ³ | Trend over the period 1953–2006 ³ |
|------|------------------------------------|---------------------|--------------------------|---------------------------------------|--|--|
| E1 | 9.4 | 5.44 | 9.0 | 7.65 | -0.019 ± 0.008 | -0.013 ± 0.005 |
| E2 | 8.8 | 3.24 | 7.79 | 5.46 | -0.041 ± 0.014 | -0.019 ± 0.004 |
| E3 | 8.0 | 2.08 | 6.80 | 3.01 | -0.038 ± 0.021 | -0.023 ± 0.007 |
| E4 | 8.5 | 1.96 | 7.06 | 2.92 | -0.064 ± 0.020 | -0.032 ± 0.017 |
| E5 | 7.4 | 0.62 | 4.76 | 0.36 | -0.087 ± 0.030 | -0.063 ± 0.011 |

¹ Ice extent is defined as the total oceanic area with an ice concentration of at least 15%.

² In this experiment, scenario SRES B1 is used.

³ This represents the mean trend over the ensemble performed for each parameter set (in 10^6 km² per decade). The uncertainty is measured as one standard deviation of the ensemble. The observed value for this trend is $0.060 \pm 0.010 \times 10^6$ km² per decade for the period 1979–2006 and $0.051 \pm 0.004 \times 10^6$ km² per decade for the period 1953–2006 (Stroeve et al., 2007).

[Title Page](#)
[Abstract](#)
[Introduction](#)
[Conclusions](#)
[References](#)
[Tables](#)
[Figures](#)
[Back](#)
[Close](#)
[Full Screen / Esc](#)
[Printer-friendly Version](#)
[Interactive Discussion](#)

Summer sea ice during the early Holocene

H. Goosse et al.

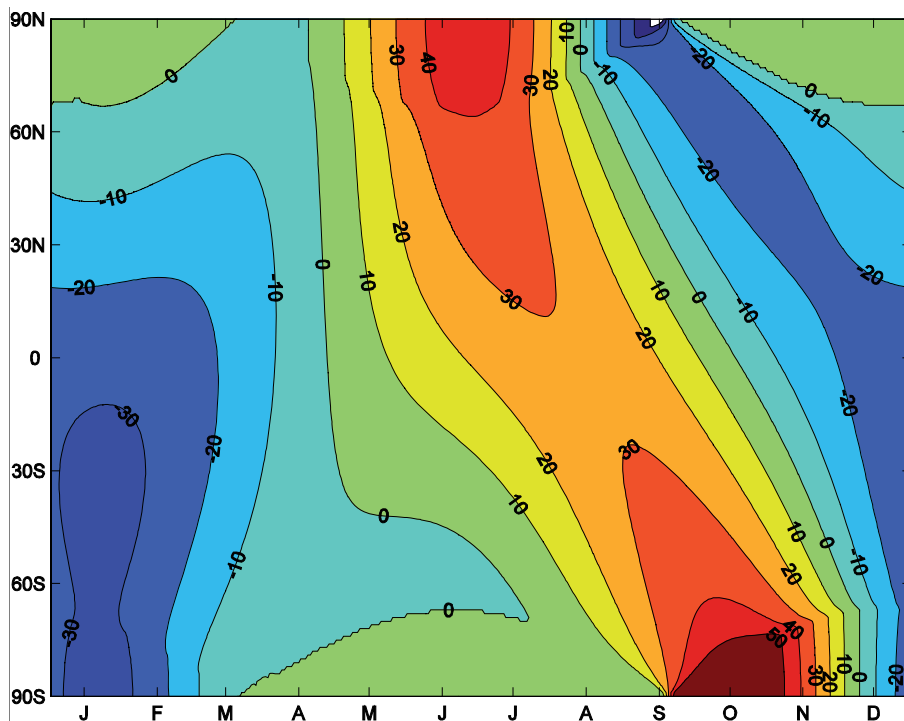


Fig. 1. Deviations from present-day values of the calendar 24 h mean irradiance (daily insolation) at 8 kyr BP (unit is Wm^{-2}).

[Title Page](#)[Abstract](#)[Introduction](#)[Conclusions](#)[References](#)[Tables](#)[Figures](#)[◀](#)[▶](#)[◀](#)[▶](#)[Back](#)[Close](#)[Full Screen / Esc](#)[Printer-friendly Version](#)[Interactive Discussion](#)

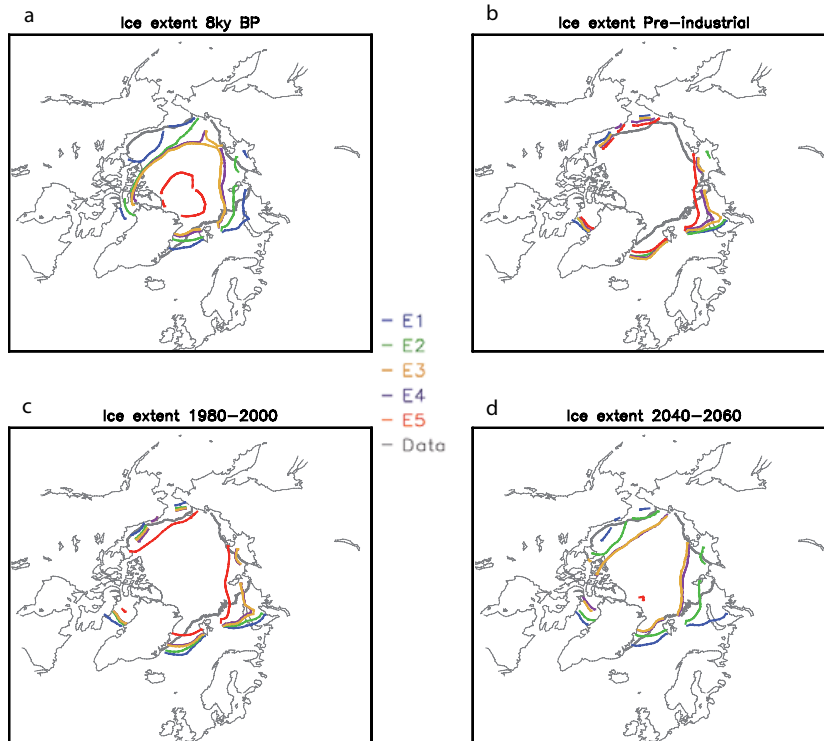


Fig. 2. Location of the sea ice edge in September, defined as the 15% ice concentration limit. For **(a)** 8 kyr BP, **(b)** pre-industrial conditions, **(c)** the period 1980–2000 AD and **(d)** the period 2040–2060 AD in scenario SRES B1, E1 is in blue, E2 in green, E3 in orange, E4 in violet and E5 in red. The observed ice edge for the period 1980–2000 AD (Comision 1999 updated 2005) is in grey on all the figures for an easier reference. For the periods 1980–2000 and 2040–2060, the mean over the 5 ensemble members using the same parameter set is presented. For pre-industrial and early Holocene, a 100 years mean is displayed.

Title Page

Abstract

Introduction

Conclusions

References

Tables

Figures

◀

▶

◀

▶

Back

Close

Full Screen / Esc

Printer-friendly Version

Interactive Discussion

Arctic – september sea ice extent

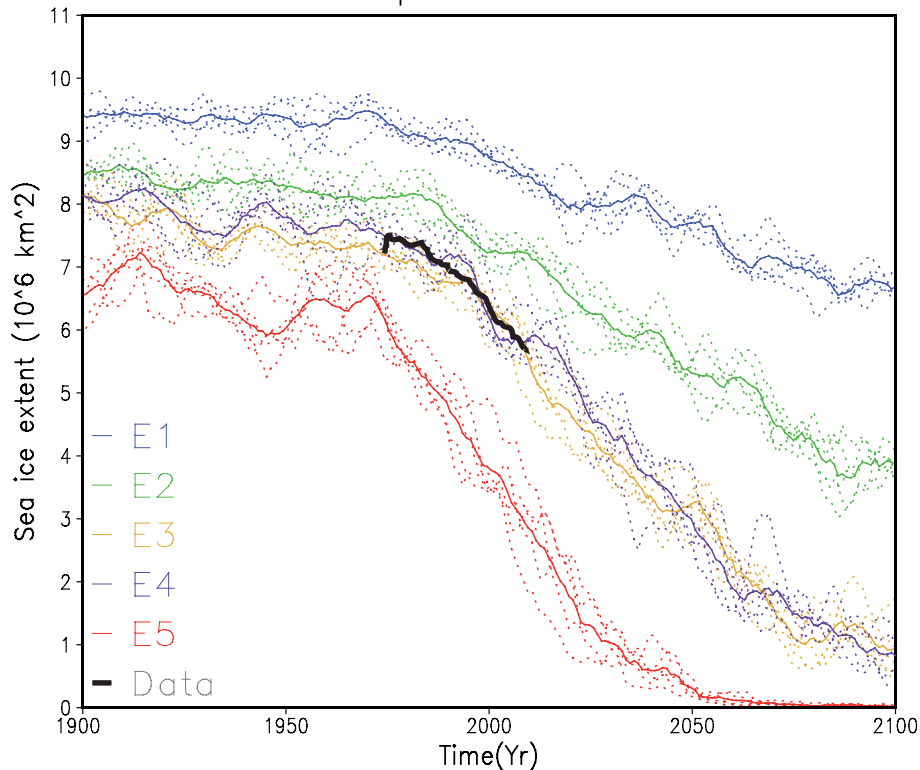


Fig. 3. Time evolution of the minimum ice extent in the Arctic over the period 1900–2100 AD using scenario SRES B1. Each simulation is represented by a dashed line while the mean over the 5 simulations with the same parameter sets is represented by a solid line of the same colour. The observations (Stroeve et al. 2007) are in black. A 11-year running mean has been applied to the time series.

Title Page

Abstract

Introduction

Conclusions

References

Tables

Figures

◀

▶

◀

▶

Back

Close

Full Screen / Esc

Printer-friendly Version

Interactive Discussion

Summer sea ice during the early HoloceneH. Goosse et al.

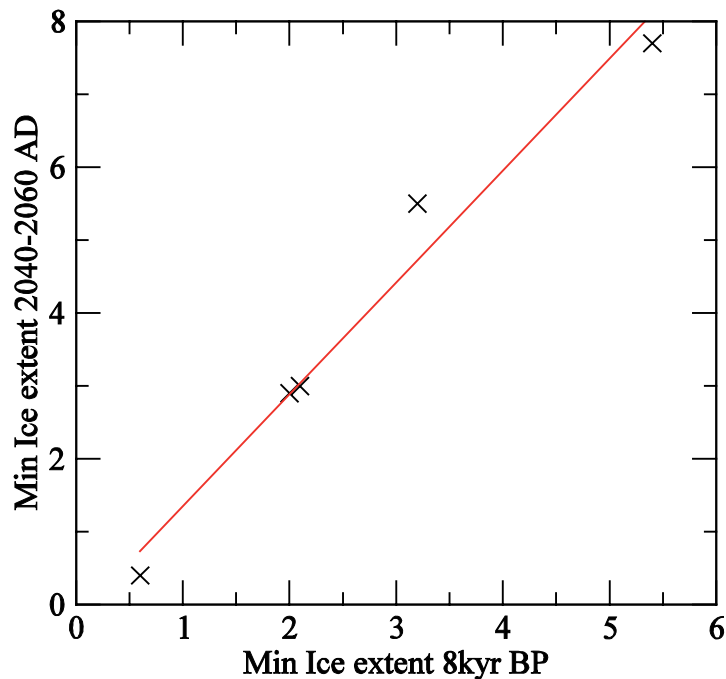


Fig. 4. Link between the minimum Arctic sea ice extent (in 10^6 km^2) for the early Holocene and the period 2040–2060 AD using scenario SRES B1. Simulations corresponding to different parameter sets (E1 to E5) are represented by a cross. The red line is a regression line for those five points.

[Title Page](#)[Abstract](#)[Introduction](#)[Conclusions](#)[References](#)[Tables](#)[Figures](#)[◀](#)[▶](#)[◀](#)[▶](#)[Back](#)[Close](#)[Full Screen / Esc](#)[Printer-friendly Version](#)[Interactive Discussion](#)

Arctic – september sea ice extent

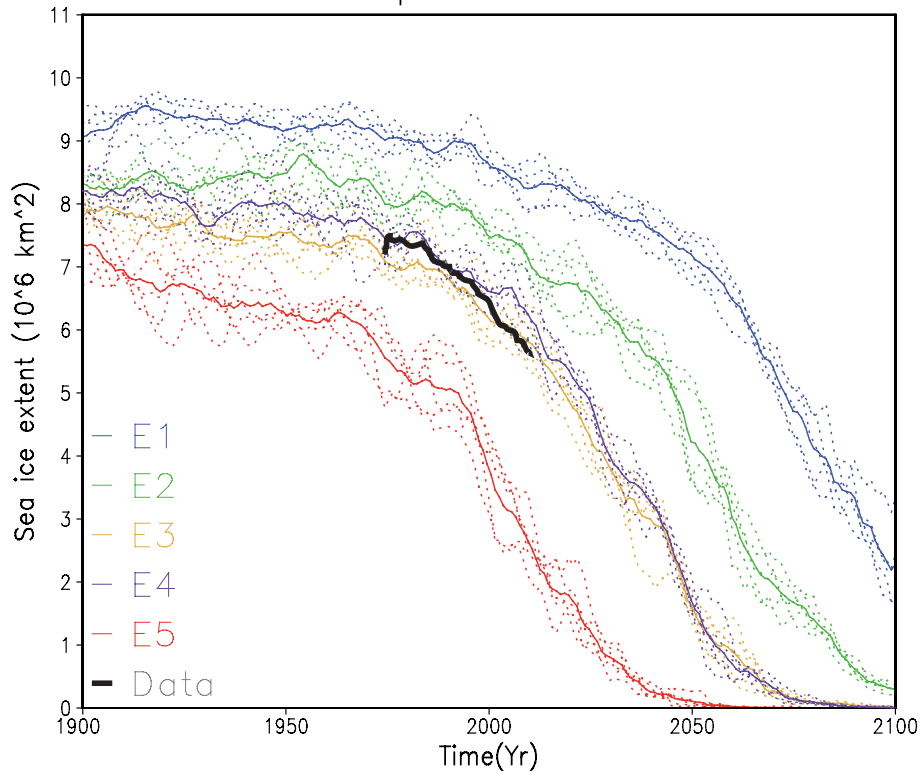


Fig. 5. Time evolution of the minimum ice extent in the Arctic over the period 1900–2100 AD using scenario SRES A2. Each simulation is represented by a dashed line while the mean over the 5 simulations with the same parameter sets is represented by a solid line of the same colour. The observations (Stroeve et al., 2007) are in black. A 11-year running mean has been applied to the time series.

Title Page

Abstract

Introduction

Conclusions

References

Tables

Figures

◀

▶

◀

▶

Back

Close

Full Screen / Esc

Printer-friendly Version

Interactive Discussion